Sonochemical synthesis and resonance light scattering effect of Zn(II)bis(1-(2-pyridylazo)-2-naphthol) nanorods

2007 Nanotechnology 18 195606

(http://iopscience.iop.org/0957-4484/18/19/195606)

IOP PUBLISHING NANOTECHNOLOGY
Nanotechnology **18** (2007) 195606 (6pp) doi:10.1088/0957-4484/18/19/195606

Sonochemical synthesis and resonance light scattering effect of Zn(II)bis(1-(2-pyridylazo)-2-naphthol) nanorods

Hong-Cheng Pan[1], **Fu-Pei Liang**[1,2,3], **Chang-Jie Mao**[1] **and Jun-Jie Zhu**[1,3]

[1] Key Lab of Analytical Chemistry for Life Science (MOE), School of Chemistry and Chemical Engineering, Nanjing University, Nanjing 210093, People's Republic of China
[2] School of Chemistry and Chemical Engineering, Guangxi Normal University, Guilin 541004, People's Republic of China

E-mail: jjzhu@nju.edu.cn

Received 8 November 2006, in final form 18 March 2007
Published 17 April 2007
Online at stacks.iop.org/Nano/18/195606

Abstract
Zn(II)bis(1-(2-pyridylazo)-2-naphthol) ($Zn(PAN)_2$) complex nanorods have been successfully synthesized via a facile sonochemical method. The transmission electron microscopy (TEM) images showed that the products had a rod-like morphology with a diameter of about 20–70 nm and a length of about 100–300 nm. The $Zn(PAN)_2$ nanorods exhibit an intense resonance light-scattering (RLS) effect, displaying a very strong RLS peak at 622 nm, a moderate peak at 361 nm and several broad bands ranged from 400 to 550 nm. The effect of ultrasonic irradiation and the mechanism of aggregation growth and resonance-enhanced light scattering were also discussed. Exciton coupling among neighbour $Zn(PAN)_2$ complex monomers in the nanorods were found to produce resonance-enhanced light scattering. The red-shifted absorption bands and depolarized RLS data can be explained in terms of a J-aggregate geometry of $Zn(PAN)_2$.

1. Introduction

Although fluorescent nanoparticles have been extensively applied in molecular biology [1–4], little attention was devoted to developing the functional nanoparticles for light-scattering applications in the fields of biological labelling, imaging and ultrasensitive assays. This is partially due to the fact that the conventional light-scattering techniques usually do not involve the absorption of nanoparticles. In this case, the scattered light intensity is proportional to the inverse fourth power of the incident light wavelength (λ) (Rayleigh's law). Disadvantages of this λ^{-4}-dependent light scattering are that it is not suitable for multicolour and multiplexing applications, and the scattered light intensity sharply decreases in the near-infrared wavelength region in which there is a good optical window for biomolecular detection. However, when the wavelength of incident light is at or near the absorption band of the particles, the light-scattering intensity deviates from Rayleigh's law and a drastic enhancement of scattered light, termed resonance light scattering (RLS), would be observed [5–7]. The RLS profile shows a wavelength-dependent characteristic of the absorption spectrum of the scattering aggregates. A quantum mechanical model demonstrate that RLS intensity is highly sensitive to exciton-coupled aggregates; but only those particles in size from nanometre-to-micrometre are likely to yield strong RLS signatures [6]. In the past few years, RLS has attracted considerable attention from both fundamental and applied research. Recently, several groups have shown that some metal and semiconductor nanoparticles, such as Au, Ag and HgS, could be used as RLS probes in biosensing applications [9–14].

Due to the existence of strong exciton coupling between neighbouring monomers, metal–chromophore complex

[3] Authors to whom any correspondence should be addressed.

nanoparticles exhibit excellent RLS properties and are becoming increasingly attractive. Indeed, highly polarizable π-electron conjugated metal–chromophore complexes lend themselves to be very promising candidates for nonlinear optical applications, such as optical switching and optical limiting devices [15]. However, the preparation of well-defined metal–chromophore nanoparticles has remained a challenge over the years. In our previous work, we have concentrated on the applications of the sonochemical approach to the synthesis of inorganic nanoparticles with different morphologies, such as heterostructured Bi_2Se_3 nanowires, CdSe hollow spherical assemblies, $BiPO_4$ nanorods, $PbWO_4$ nanocrystals, Bi_2S_3 nanorods, gold nanorings, $Cd(OH)_2$ nanorings and self-assembled V_2O_5 bundles [16–23]. Herein, we describe a novel sonochemical approach to prepare the metal–chromophore complex Zn(II)bis(1-(2-pyridylazo)-2-naphthol) ($Zn(PAN)_2$) nanorods with strong RLS property. To our knowledge, a sonochemical synthesis of $Zn(PAN)_2$ nanorods has not been achieved previously. The sonochemical method presented here is feasible, rapid, mild and energy efficient. The as-prepared $Zn(PAN)_2$ nanorods were investigated by elemental analysis (EA), Fourier transform infrared (FT-IR), transmission electron microscopy (TEM) and RLS properties of the nanorods have been studied. The RLS spectrum of $Zn(PAN)_2$ nanorods displays that there is a strong RLS peak centred at 622 nm and a moderate RLS peak centred at 361 nm. The mechanism of resonance-enhanced light scattering has been investigated.

2. Experimental section

2.1. Materials

1-(2-pyridylazo)-2-naphthol (PAN) was purchased from Shanghai No. 1 Chemicals Factory (China). Zinc acetate was purchase from Beijing Chemical Reagents Company (China). All the reagents used were of analytical purity and used without further purification. Doubly distilled water was used throughout.

2.2. Preparation of the Zn(PAN)$_2$ nanorods

The $Zn(PAN)_2$ nanorods were prepared by using a sonochemical route. 1 mmol of 1-(2-pyridylazo)-2-naphthol was dissolved in 60 ml of 50% (v/v) ethanol aqueous solution and 2 ml of 25% (w/w) ammonia solution was added. 0.2 mmol of zinc acetate was dissolved in 60 ml of 50% (v/v) ethanol aqueous solution and then was added to the above solution. The mixture solution was exposed to high-intensity ultrasound irradiation under ambient air for 60 min. Ultrasound irradiation was accomplished with a high-intensity ultrasonic probe (Xinzhi Co., Xinzhi, China; 1.2 cm diameter; Ti horn, 20 kHz, 100 W cm^{-2}) immersed directly in the reaction solution. When the reaction was finished, a dark red-brown precipitate was obtained. After cooling of the sample to room temperature, the precipitate was separated by centrifuging at a rotation rate of 9000 rounds min^{-1}. The precipitate was purified further by repeated cycles of centrifuging and dispersing in ethanol and diluted ammonia aqueous solution and then was dried in air at room temperature. The final products were re-dispersed in 50% (v/v) glycerol/water solution for further usage.

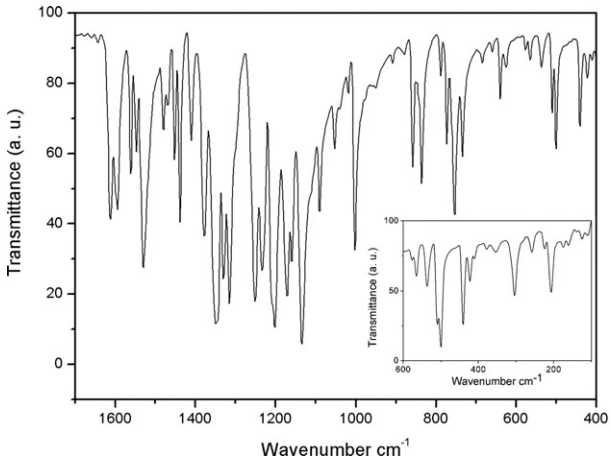

Figure 1. IR spectrum of the $Zn(PAN)_2$ nanorods. Inset: far-IR spectrum.

2.3. Characterization

UV–vis absorption spectra were recorded with a Shimadzu UV-3600 UV–vis–NIR spectrophotometer. The infrared (IR) and FTIR spectra were obtained using a Nicolet Nexus 870 FT-IR spectrophotometer. Elemental analysis (EA) was carried out using a Heraeus CHN-O Rapid instrument. The transmission electron microscopy (TEM) was performed on a JEOL JEM-200CX microscope. The resonance light scattering was recorded on a Hitachi 850 Fluorescence spectrophotometer at a 90° scattering angle. The resonance light scattering (RLS) spectra were obtained by synchronously scanning the excitation and emission monochromators in the wavelength region from 300 to 700 nm (namely, $\lambda_{ex} = \lambda_{em}$). The depolarization ratio of scattered light is measured according to the literature [7]. For vertically polarized exciting radiation and scattered radiation detected at 90°, the depolarization ratio is defined as $\rho_V(90) = G \cdot I_{VH}/I_{VV}$, where I_{VH} is the scattered intensity with horizontal polarization, I_{VV} is the scattered intensity with vertical polarization and $G = I_{HV}/I_{HH}$ is the correction factor. All spectra were collected at room temperature.

3. Results and discussion

3.1. Structure and morphology

The EA of the sample shows that the content (%) of C, N and H is 64.12, 14.80 and 3.41, respectively. The values are consistent with the calculated values (C: 64.12%; N: 14.96%; H: 3.59%) and the product can be confirmed to be $Zn(PAN)_2$. Figure 1 shows the IR spectrum of the as-prepared $Zn(PAN)_2$ nanorods. The band positions are consistent with previous reports on $Zn(PAN)_2$ complex [24]. In the IR region between 1700 and 400 cm^{-1}, the peaks are attributed to the PAN ligand vibrations, and in the far-IR region between 400 and 100 cm^{-1}, the metal–ligand vibrations are observed. The detailed assignments are summarized in table 1. According to the data of IR and EA, the composition of the product can be confirmed as $Zn(PAN)_2$. The size and morphology of the $Zn(PAN)_2$ nanorods were examined by TEM (transmission

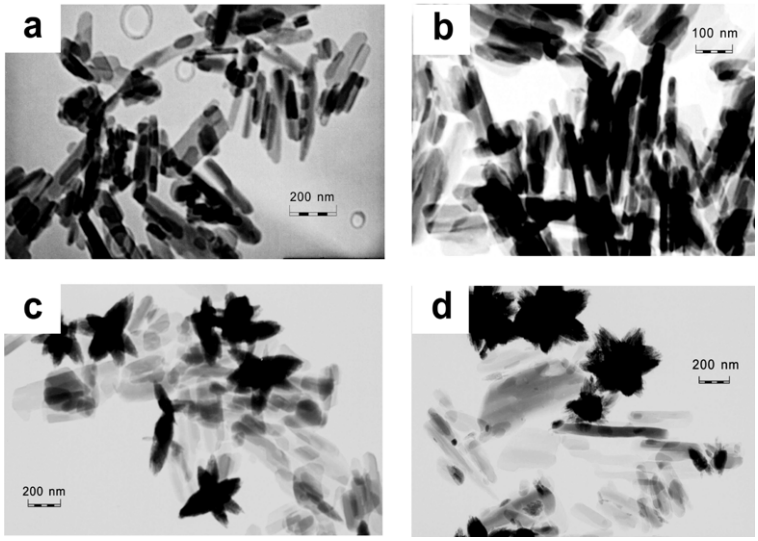

Figure 2. TEM images of as-prepared products under different molar ratios of PAN:Zn(II) (a) 5:1; (b) 1:1; (c) 1:5 and (d) 1:10.

Table 1. Wavenumbers and assignments of IR spectra of the $Zn(PAN)_2$ nanorods (abbreviations: ν—stretching mode; δ—bending mode; a—azo, p—pyridine; n—naphthol).

Wavenumbers (cm^{-1})	Assignment	Wavenumbers (cm^{-1})	Assignment	Wavenumbers (cm^{-1})	Assignment
1612	$\nu(CC)_n + \nu(CN)$	1234	$\delta(CH)$	624	$\delta(CCC)_n + \nu(CC)_n + \delta(CO)$
1595	$\nu(CC)_p + \nu(CC)_n$	1202	$\nu(CC)_n$	575	$\delta(CCC)_p + \delta(CCC)_n$ $+\nu(C_nN) + \nu(C_pN)$
1562	$\nu(CC)_p$	1170	$\nu(CC)_p + \nu(CN)_n$ $+\nu(NN)$	563	$\delta(CCC)_n + \nu(CC)_n$
1548	$\nu(CC)_n$	1159	$\nu(CC)_p + \nu(CN)_n$ $+\nu(NN)$	536	$\delta(CCC)_n + \nu(CC)_n$
1529	$\nu(CC)_n$	1134	$\nu(CC)_p + \delta(CCC)_p$	509	$\delta(CNNC)_p + \delta(ZnN_aN)n$ $+\delta(COZn)$
1479	$\delta(CH) + \nu(CC)$	1089	$\nu(CC)_n + \nu(NN)$	500	$\delta(CNNC)_p + \delta(ZnN_aN)n$ $+\delta(COZn)$
1468	$\delta(CH) + \nu(CC)$	1053	$\delta(CH)$	440	$\delta(CCC)_n$
1452	$\delta(CH) + \nu(CC)$	1001	$\nu(CC)_p + \delta(CC)_p$ $+\nu(C_pN)$	422	$\delta(CCC)_n$
1438	$\delta(CH) + \nu(CC)$	858	$\delta(CH)$	378	$\delta(CCC)_n + \nu(ZnO)$
1409	$\nu(CC)_n + \nu(C_nN)$	837	$\nu(CC)_p + \delta(CCC)_p$ $+\nu(C_pN)$	353	$\delta(CCC)_n + \nu(ZnO)$
1377	$\nu(CC)_n + \nu(C_pN)$	788	$\delta(CH) + \delta(CCC)$	305	$\delta(CCC)_n + \nu(ZnO)$
1348	$\nu(CC)_n + \nu(CN)_n$ $+\nu(C_pN) + \nu(C_nN)$	773	$\delta(CH) + \delta(CCC)$	258	$\nu(ZnN_p) + \nu(ZnO)\delta(N_aZnO)$ $+\delta(ZnN_aN)n$
1330	$\nu(NN) + \nu(CC)_n$ $+\nu(CO)$	754	$\delta(CH) + \delta(CCC)$	224	$\delta(CNNC) + \nu(ZnN_p)$ $+\nu(ZnO) + \nu(ZnN_a)$
1315	$\nu(NN) + \nu(CC)_n$ $+ \nu(CO)$	733	$\delta(CCC)_p + \nu(CC)_n$ $+\delta(CNNC)$	208	$\delta(N_aZnO) + \delta(ZnN_pC) + \nu(ZnO)$ $+\nu(ZnN_a) + \nu(ZnN_p)$
1251	$\nu(CC)_p + \nu(C_nN)$	638	$\delta(CCC)_p$	175	$\delta(N_aZnO) + \delta(ZnN_pC)$ $+\nu(ZnO) + \nu(ZnN_a) + \nu(ZnN_p)$

electron microscope). A typical TEM image shown in figure 2(a) reveals that the as-prepared $Zn(PAN)_2$ nanoparticles present a rod-like morphology with a diameter of 20–70 nm and a length of 100–300 nm.

3.2. UV–vis spectra of $Zn(PAN)_2$ nanorods

Transition moment coupling of strongly absorbing chromophores can result in dramatic perturbations to the UV–vis spectra of dimers and higher aggregates [25]. Figure 3 compares the absorption spectra of $Zn(PAN)_2$ nanorods in 20 mM NaAc–HAc buffer solution (pH = 4.2, containing 3 wt% glycerol) (solid line), $Zn(PAN)_2$ dissolved in carbon tetrachloride/acetone (1:3, v/v) (dashed line) and PAN dissolved in carbon tetrachloride/acetone (1:3, v/v) (dotted line). The absorption spectra of the $Zn(PAN)_2$ sample dissolved in carbon tetrachloride/acetone solution is used to represent the $Zn(PAN)_2$ monomer. Resonance light scattering measurements presented below also support this conclusion. As shown in figure 3, due to intramolecular charge transfer, the absorption maximum of PAN at 464 nm is red-shifted to 554 nm, where

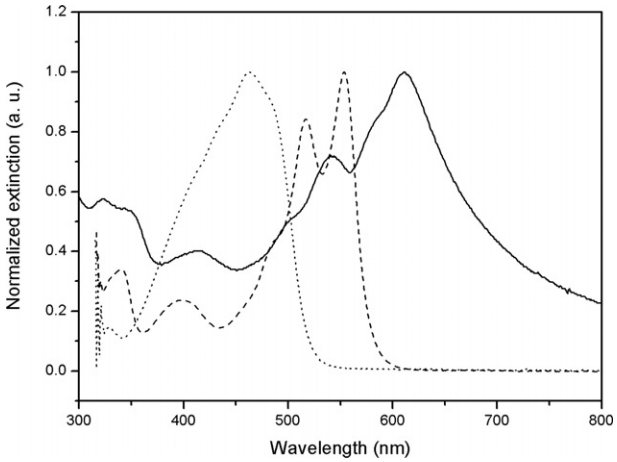

Figure 3. Absorption spectra of $Zn(PAN)_2$ nanorods in 20 mM NaAc–HAc buffer solution (pH = 4.2, containing 3 wt% glycerol) (solid line), $Zn(PAN)_2$ in carbon tetrachloride/acetone (1:3, v/v) (dashed line) and PAN in carbon tetrachloride/acetone (1:3, v/v) (dotted line).

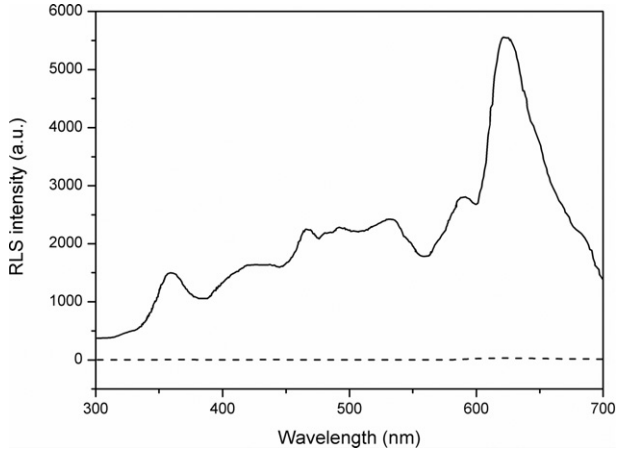

Figure 4. RLS spectra of $Zn(PAN)_2$ nanorods dispersion at pH 4.2 (solid line). Dashed line represent RLS spectrum of $Zn(PAN)_2$ dissolved in carbon tetrachloride/acetone (1:3, v/v).

$Zn(PAN)_2$ monomer absorption is maximum. The dispersion of the $Zn(PAN)_2$ nanorods displayed an absorption maximum at 611 nm, a shoulder peak at 542 nm, a weak peak at 414 nm, a weak shoulder peak at 348 nm and a moderately intense peak at 323 nm. The $Zn(PAN)_2$ nanorods exhibited red-shifted absorption bands with respect to $Zn(PAN)_2$ monomer absorption. It is generally accepted that the usual model for describing intermolecular interactions invokes the concept of H- and J-aggregates of dipole-coupled chromophore-aggregates [26]. The most characteristic feature of J-aggregates is the red-shifted absorption band (J-band) with respect to the monomer absorption, in contrast to the blue-shifted absorption band for H-aggregates [27]. In the case of $Zn(PAN)_2$ nanorods, the red-shifted absorption bands indicate that these $Zn(PAN)_2$ monomers may interact with each other in an J-aggregate fashion, where the transition moments of monomers are aligned parallel to the line joining their centres in an end-to-end stacking mode [28].

3.3. Resonance light scattering properties of Zn(PAN)$_2$ nanorods

When irradiating a solution of chromophore aggregates with an electromagnetic field close to the absorption frequency, the electric field is highly localized and consequently leads to strong collective spatial fluctuations [29]. In this case, the intensity of scattered light is resonance-enhanced by several orders of magnitude because of excitonic coupling among transition dipoles on neighbouring chromophores [5–7]. The RLS phenomena were observed in many cases [30–34]. In this present study, the as-prepared $Zn(PAN)_2$ nanorods exhibited a strong RLS effect. Figure 4 shows the RLS spectra of the $Zn(PAN)_2$ nanorods. A very strong RLS peak at 622 nm, a shoulder peak 589 nm and a moderate peak at 361 nm were observed (solid line in figure 4). Also, it could be seen that there were several broad bands in the wavelength range from 400 to 550 nm. The intense RLS signal suggests that this $Zn(PAN)_2$ complex forms an aggregate with a large aggregation number and exciton coupling exists between neighbour $Zn(PAN)_2$ complex monomers. In contrast, $Zn(PAN)_2$ complex monomers or small oligomers, which could be obtained by dissolving the sample in carbon tetrachloride/acetone (1:3, v/v) solution, do not show such enhanced light scattering (dashed line in figure 4). The theory of RLS demonstrated that the resonance light scattering profile has a wavelength-dependent characteristic of the absorption spectrum of the scattering aggregates [6]. In the case of $Zn(PAN)_2$ nanorods, the RLS peaks at 622, 589 and 361 nm correspond to the absorption peak at 611, 542 and 323 nm, respectively. The RLS peaks were found to be slightly red-shifted from the absorption bands. Analogous phenomena also have been reported on other chromophore aggregates [22].

As demonstrated by the quantum mechanical model, the value of the depolarization ratio ($\rho_V(90)$) measured at the resonance frequency reports directly on the geometry of the excited state of the aggregate, regardless of its size [8]. The value of $\rho_V(90)$ has been calculated for three limiting cases: (1) an aggregate with a spherically symmetric tensor has $\rho_V(90) = 0$; (2) an aggregate with one nondegenerate excited state has $\rho_V(90) = 1/3$; and (3) an aggregate with a degenerate excited state has $\rho_V(90) = 1/8$. Furthermore, the $\rho_V(90)$ value of slipped J-aggregates is expected ranging from 1/8 to 1/3. In this study, the depolarization ratio of the $Zn(PAN)_2$ nanorods was measured at maximum RLS wavelength (622 nm) with a value of 0.23. The depolarized RLS data, combined with resonance-enhanced light scattering and red-shifted absorption bands, supported a J-aggregate geometry for $Zn(PAN)_2$ nanorods [30–32, 34]. The structure of J-aggregates are assemblies of noncovalently coupled $Zn(PAN)_2$ monomers in the form of linear or circular chains, which, in turn, can form complex cylindrical patterns. The macroscopic appearance of the J-aggregates that would be a rod-like morphology is consistent with the TEM images shown in figure 2(a).

3.4. Effect of synthetic conditions

A variety of synthetic conditions have been examined for the preparation of $Zn(PAN)_2$ nanorods. Zn(II) was chelated with

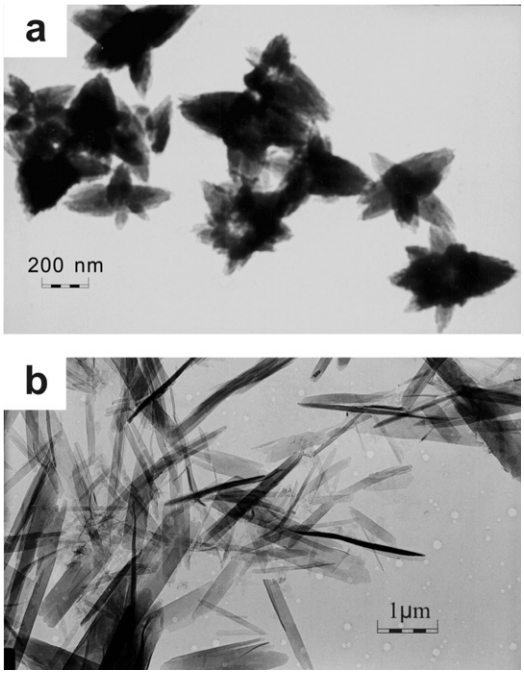

Figure 5. TEM images of samples prepared under different conditions: (a) without PAN and (b) without ultrasound.

PAN to yield a $Zn(PAN)_2$ complex in alkaline solution. In this study, 2 ml ammonia aqueous solution (25 wt%) was added to maintain an alkaline reaction environment. However, no significant changes were observed with the addition of ammonia aqueous solution up to 5 ml. Figure 2 shows the TEM images of as-prepared $Zn(PAN)_2$ nanorods under the molar ratios of PAN:Zn(II) in the range from 5:1 to 1:10. It was found that the molar ratio of PAN:Zn(II) between 5:1 and 1:1 favoured the growth of $Zn(PAN)_2$ complex to pure and uniform nanorods. When the ratio is reduced, the as-prepared $Zn(PAN)_2$ nanorods maintained the same morphology, but the sizes are found to increase slightly. Figure 2(b) shows the TEM images of a sample when the molar ratio is 1:1. Lower molar ratios of PAN:Zn(II) were also tried. In this case, excessive Zn(II) hydrolyzed in alkaline reaction solution and formed petal-shaped $Zn(OH)_2$ nanocrystals. When the ratios of PAN:Zn(II) are 1:5 and 1:1, as shown in figure 2(c) and (d), there are two types of morphology: one is nanorods which corresponded to $Zn(PAN)_2$ and the other is a petal-like nanostructure which is attributed to $Zn(OH)_2$. The above conclusion is supported by the results that single petal-like morphology could be obtained, as shown in figure 2(e), under the identical synthetic conditions except without the addition of PAN. The x-ray powder diffraction (XRD) results indicated that the product was $Zn(OH)_2$.

3.5. Effect of ultrasonic irradiation and possible growth mechanism

It has been well established that the ultrasonic irradiation introduces a variety of physical and chemical effects deriving from acoustic cavitation [35]. Such cavitation behaviour, i.e. the formation, growth and implosive collapse of bubbles, has been used extensively to generate novel materials with unusual properties. Comparative experiments under vigorous electric stirring instead of ultrasonic treatment only obtained irregular flakes on the several-micrometres scale (figure 5(b)). The growth mechanism of $Zn(PAN)_2$ nanorods is similar to the mechanism reported in the literature [36, 37]. The probable reaction process for the sonochemical formation of $Zn(PAN)_2$ nanorods can be summarized as follows. Initially, the complexing action between Zn(II) and PAN leads to the formation of a $Zn(PAN)_2$ complex. It was found that the small $Zn(PAN)_2$ nuclei could be formed in the presence of ultrasound. Under the microjets and shockwaves formed at the collapse of the bubbles, the nuclei are pushed towards each other. The nanorods are formed as a result of the interparticle collisions. During the interparticle collisions, the particles can be driven together at sufficiently high speeds to induce effective melting at the point of collision. In the growth process, $Zn(PAN)_2$ nanoparticles present a preferential directional growth due to its inherent anisotropic structure. As a result, the product presents a rod-type morphology. This idea of nanoparticles created at the early stages of the sonochemical reaction and further colliding to form nanorods has been used for the explanation of the sonochemical formation of Bi_2S_3, Sb_2S_3 and Eu_2O_3 nanorods [20, 36, 37].

4. Conclusion

Metal–chromophore complex $Zn(PAN)_2$ nanorods have been successfully synthesized via a facile sonochemical route. The experimental results showed that ultrasonic irradiation played a key role for the formation of uniform nanorods. A strong RLS phenomenon was observed from the $Zn(PAN)_2$ nanorods' dispersion. The existence of an excitonically coupled (delocalized) electronic transition is revealed by strong RLS signals which are slightly red-shifted from the absorption band. We deduce that the aggregation of $Zn(PAN)_2$ can yield a J-aggregate. This assessment is supported by the red-shifted absorption band with respect to the monomer, which is characteristic for J-aggregate formation, and depolarized RLS data which are consistent with a slipped J-aggregate. Furthermore, rod-like morphology of the J-aggregate are revealed by TEM, indicating linear stacking of the $Zn(PAN)_2$ molecules in the J-aggregate.

Acknowledgments

We greatly appreciate the support of the National Natural Science Foundation of China (Nos. 20325516, 20635020, 90606016, 90206037). This work is also supported by NSFC for Creative Research Group (20521503).

References

[1] Gaponik N, Radtchenko I L, Sukhorukov G B, Weller H and Rogach A L 2002 *Adv. Mater.* **14** 879
[2] Larson D R, Zipfel W R, Williams R M, Clark S W, Bruchez M P, Wise F W and Webb W W 2003 *Science* **300** 1434
[3] Wang L, Yang C and Tan W 2005 *Nano Lett.* **5** 37
[4] Ow H, Larson D R, Srivastava M, Baird B A, Webb W W and Wiesner U 2005 *Nano Lett.* **5** 113
[5] Pasternack R F and Collings P J 1995 *Science* **269** 935

[6] Pasternack R F, Bustamante C, Collings P J, Giannetto A and Gibbs E J 1993 *J. Am. Chem. Soc.* **115** 5393
[7] Collings P J, Gibbs E J, Starr T E, Vafek O, Yee C, Pomerance L A and Pasternack R F 1999 *J. Phys. Chem.* B **103** 8474
[8] Parkash J, Robblee J H, Agnew J, Gibbs E, Collings P, Pasternack R F and de Paula J C 1998 *Biophys. J.* **74** 2089
[9] Aslan K, Holley P, Davies L, Lakowicz J R and Geddes C D 2006 *J. Am. Chem. Soc.* **127** 12115
[10] Aslan K, Lakowicz J R and Geddes C D 2005 *Anal. Chem.* **77** 2007
[11] Jiang Z, Sun S, Liang A, Huang W and Qin A 2006 *Clin. Chem.* **52** 1389
[12] Wu L P, Li Y F, Huang C Z and Zhang Q 2006 *Anal. Chem.* **78** 5570
[13] Liu S P, Yang Z, Liu Z F and Kong L 2006 *Anal. Biochem.* **353** 108
[14] Wang L Y, Wang L, Dong L, Hu Y L, Xia T T, Chen H Q, Li L and Zhu C Q 2004 *Talanta* **62** 237
[15] De la Torre G, Vázquez P, Agulló-López F and Torres T 1998 *J. Mater. Chem.* **8** 1671
[16] Qiu X, Burda C, Fu R, Pu L, Chen H and Zhu J 2004 *J. Am. Chem. Soc.* **126** 16276
[17] Zhu J-J, Xu S, Wang H and Chen H-Y 2003 *Adv. Mater.* **15** 156
[18] Geng J, Hou W-H, Lv Y-N, Zhu J-J and Chen H-Y 2005 *Inorg. Chem.* **44** 8503
[19] Geng J, Zhu J-J and Chen H-Y 2006 *Cryst. Growth Des.* **6** 321
[20] Wang H, Zhu J-J, Zhu J-M and Chen H-Y 2002 *J. Phys. Chem.* B **106** 3848
[21] Jiang L-P, Xu S, Zhu J-M, Zhang J-R, Zhu J-J and Chen H-Y 2004 *Inorg. Chem.* **43** 5877
[22] Miao J-J, Fu R-L, Zhu J-M, Xu K, Zhu J-J and Chen H-Y 2006 *Chem. Commun.* 3013
[23] Mao C-J, Pan H-C, Wu X-C, Zhu J-J and Chen H-Y 2006 *J. Phys. Chem.* B **110** 14709
[24] Drozdzewski P M 1989 *Spectrochim. Acta* A **45** 455
[25] Choi M Y, Pollard J A, Webb M A and McHale J L 2003 *J. Am. Chem. Soc.* **125** 810
[26] Dautel O J, Wantz G, Almairac R, Flot D, Hirsch L, Lere-Porte J-P, Parneix J-P, Serein-Spirau F, Vignau L and Moreau J J E 2006 *J. Am. Chem. Soc.* **128** 4892
[27] Kitahama Y, Kimura Y and Takazawa K 2006 *Langmuir* **22** 7600
[28] Lim I-I S, Goroleski F, Mott D, Kariuki N Ip W, Luo J and Zhong C-J 2006 *J. Phys. Chem.* B **110** 6673
[29] Scolaro L M, Romeo A, Castriciano M A and Micali N 2005 *Chem. Commun.* 3018
[30] Kano K, Fukuda K, Wakami H, Nishiyabu R and Pasternack R F 2000 *J. Am. Chem. Soc.* **122** 7494
[31] Castriciano M A, Romeo A, Villari V, Micali N and Scolaro L M 2004 *J. Phys. Chem.* B **108** 9054
[32] De Luca G, Romeo A and Scolaro L M 2006 *J. Phys. Chem.* B **110** 14135
[33] Mazzaglia A, Angelini N, Darcy R, Donohue R, Lombardo D, Micali N, Sciortino M T, Villari V and Scolaro L M 2003 *Chem. Eur. J.* **9** 5762
[34] Castriciano M A, Romeo A, Villari V, Angelini N, Micali N and Scolaro L M 2005 *J. Phys. Chem.* B **109** 12086
[35] Suslick K S 1999 *Annu. Rev. Mater. Sci.* **29** 295
[36] Wang H, Lu Y N, Zhu J J and Chen H Y 2003 *Inorg. Chem.* **42** 6404
[37] Pol V G, Palchik O, Gedanken A and Felner I 2002 *J. Phys. Chem.* B **106** 9737